sciendo

ANNALS OF WEST UNIVERSITY OF TIMISOARA PHYSICS
Vol. LXIII, 2021

DOI: 10.2478/awutp-2021-0009

CORRELATION OF RHEOLOGICAL PROPERTIES OF FERROFLUID-BASED MAGNETORHEOLOGICAL FLUIDS USING SOME DIMENSIONLESS NUMBERS DEFINED IN MAGNETORHEOLOGY

Gheorghe-Orlando Vălu[1], Daniela Susan-Resiga[1,2]

[1]West University of Timisoara, Faculty of Physics, Bvd. V. Parvan, no. 4, 300222, Timisoara, Romania,
[2]Romanian Academy–Timisoara Branch, Bvd. M. Viteazu, no. 24, 300223, Timisoara, Romania.

Article Info

Received: 02.10.2021
Accepted: 25.10.2021

Keywords:
ferrofluid based magnetorheological fluids, master curve, yield stress

Abstract

In this paper we investigated from rheological point of view some samples of ferrofluid-based magnetorheological fluids (FF-MRFs) with different volumic fractions of Fe microparticles, but with the same ferrofluid used as carrier liquid. We correlated the dimensionless flow curves, measured at different values of the magnetic field induction, using either Mason number or Casson number. It has been shown that in this approach, data sets measured under different conditions collapse on a single curve. This master curve is useful for controlling the concentration of Fe particles, so that the magnetic and magnetorheological properties of FF-MRF to be adapted to obtain high-performance applications.

1. Introduction

Conventional MRFs are fluid materials whose physical properties can be modified / controlled under the action of a magnetic field. They consist of non-colloidal ferromagnetic particles, dispersed in a non-magnetic base liquid in a volume concentration of 10-50%. The possibility of adapting the behavior of MRFs using magnetic fields of moderate intensities motivates their use in various applications of active vibration control or torque transmission, from many branches of engineering and biomedical [1], [2], [3], [4], [5], [6], [7], [8]:

- vibration dampers for: civil applications - dampers positioned at the base of buildings and bridges, automotive - dampers for car seats; household applications - dampers for

washing machines, in sports – dampers for fitness equipment, in the medical field - dampers for intelligent prostheses for joints;

- clutches, brakes;
- polishing techniques;
- rotating seals.

Unfortunately, conventional MRFs also have some disadvantages, mainly caused by the "large" particle size. We mention only a few of them: their long-term sedimentation in the absence of continuous agitation, difficult redispersibility due to the remaining magnetic attraction between the particles, thickening during long use in the presence of strong magnetic fields, quite high abrasiveness.

Therefore, the strategies to improve MR fluids have become a priority concern for researchers over the past decades. A detailed review of these strategies is contained in [9], [10] and they refer to improving performance through new MRF formulations:

- preparing of inverse ferrofluids [11], [12], [13];
- adding of additives, surfactants, particles with the surface covered with an organic / inorganic layer [14], [15], [16];
- use of high viscosity and viscoelastic carrier liquids [17], preparation of magnetic gels [18] and magnetic elastomers;
- adaptation of particle size and concentration, preparation of bidisperse composites [19], [20], [21];
- using of particles with other morphologies than spherical ones for the preparation of MRF [22], [23], [24], [25];
- preparing of ferrofluid-based magnetorheological fluids (FF-MRFs), which exploit both the advantages of ferrofluids (kinetic stability) and conventional MRFs (strong magnetoviscous and magnetorheological effects) [3], [26].

The physical properties and flow behavior of FF-MRFs both in the absence and in the presence of the magnetic field have been investigated in numerous papers [27], [28], [29], [25], [30], [31], [32], [33], demonstrating the advantages of replacing conventional MRFs with FF-MRFs in practical applications.

Analyzing three sets of FF-MRF with different volume fractions of magnetite nanoparticles and Fe microparticles, based on the approximation of the average magnetization, in the paper [32] we obtained a master curve representing the dimensionless viscosity curves (measured at different values of the applied magnetic field induction) vs. the Mason number.

For the same three sets of nano-microstructured MRFs, representing the static yield stress depending of characteristic magnetic stress, in the work [33] a master curve was also generated.

The purpose of this paper is to obtain a master curve by representing the flow curves (measured for an FF-MRF at different values of the magnetic field induction) normalized with the yield stress vs. Mason number. Also, for FF-MRF samples with different volumetric fractions of Fe microparticles (but with the same ferrofluid used as carrier liquid), we aim to show that representing the dimensionless flow curves depending on the inverse of Casson number, also the data will collapse on a master curve.

2. Theory - Dimensionless shear stress master curves according to Mason number

The dynamic yield stress is defined as the stress required for materials to stop the flowing of the fluid, it marks the transition between viscoplastic and solid materials. Practicaly, it is the minimum shear stress to maintain the flow after the thixotropic structure has been destroyed [28].

The dynamic yield stress can be determined by fitting the flow curve or viscosity curve with a constitutive model that predicts the existence of dynamic yield stress, such as: Bingham, Casson or Herschel-Bulkley models.

1) For conventional MRFs (containing only one-dimensional, micrometric magnetizable particles dispersed in a non-magnetizable carrier liquid), the flow curves at high shear rates are generally linear, so they are well correlated with *Bingham's formula* [34]:

$$\tau = \tau_B + \eta_B \cdot \dot{\gamma}, \tag{1}$$

where: τ_B = the Bingham yield (stress) point,

η_B = the Bingham viscosity (a calculated coefficient also called the "Bingham flow coefficient").

Physical significance of Bingham viscosity:

To determine the physical significance of Bingham viscosity we divide formula (1) by $\dot{\gamma}$ and we obtain:

$$\eta = \frac{\tau_B}{\dot{\gamma}} + \eta_B \tag{2}$$

For very high shear rates:

$$\dot{\gamma} \to \infty \;\Rightarrow\; \eta_\infty = \eta_B \tag{3}$$

So *the Bingham viscosity represents the viscosity at infinitely high shear rates.*

Dividing equation (1) by τ_B, it results:

$$\frac{\tau}{\tau_B}=1+\frac{\eta_B}{\tau_B}\cdot\dot{\gamma} \tag{4}$$

In the case of very low magnetic field strengths in dilute suspensions, the Mason number, which is defined as the ratio of the hydrodynamic Stokes force and the magnetic polarization force, is given by the expression [35]:

$$M_{nL}=\frac{8\eta_{CL}\dot{\gamma}}{\mu_o\,\mu_{r\,CL}\,\beta^2H^2}\ , \quad \text{with} \tag{5}$$

$$\beta=\frac{\mu_{r\,p}-\mu_{r\,CL}}{\mu_{r\,p}+2\,\mu_{r\,CL}} \tag{6}$$

The meaning of physical quantities in this expressions: η_{CL} is the viscosity of the carrier liquid (which is non-magnetizable for conventional MRFs), $\dot{\gamma}=$ the shear rate, $\mu_0=4\cdot\pi\cdot10^{-7}\ {}^{N}\!/_{A^2}=$ the free space magnetic permeability, $\mu_{r\,CL}$ = the relative permeability of the carrier liquid, $\mu_{r\,p}=$ the relative permeability of the particles, $\beta=$ the coupling parameter (or contrast factor).

For very large magnetic field strengths, when the suspension compppletely magnetize, equations (5) and (6) do not apply anymore, and the Mason number becomes:

$$M_{nsat}=\frac{72\eta_{CL}\dot{\gamma}}{\mu_o\,\mu_{r\,CL}\,M_{psat}^2}\ , \tag{7}$$

where M_{psat} represents the magnetization of the particle under saturation conditions.

Using *the approximation of the average magnetization*, Klingenberg obtained a unique expression of M_n, valid for both weak and intense magnetic fields [36] in case of conventional MRFs:

$$M_n=72\frac{\eta_{CL}}{\mu_o\,\mu_{r\,CL}\left\langle M_p\right\rangle^2}\dot{\gamma} \tag{8}$$

$\left\langle M_p\right\rangle=$ the average magnetization of a spherical particle from MRF. The Mason number allows to describe the dependence of the viscosity of MRF simultaneous on both the shear rate and the magnetic induction of the applied field by using only this one variable, M_n.

Knowing average magnetization $\langle M_{MRF} \rangle$ of MRF and volume fraction Φ of particles dispersed in the MRF, $\langle M_p \rangle$ is determined by the formula:

$$\langle M_p \rangle = \frac{\langle M_{MRF} \rangle}{\Phi} \tag{9}$$

The critical Mason number is defined as the Mason number for a critical shear rate value $\left(\dot{\gamma} = \frac{\tau_B}{\eta_\infty} \right)$:

$$M_n^* = 72 \frac{\eta_{CL}}{\mu_o \, \mu_{rCL} \langle M_p \rangle^2} \cdot \frac{\tau_B}{\eta_\infty} \tag{10}$$

It follows from (8) and (10):

$$\frac{M_n}{M_n^*} = \frac{\eta_\infty}{\tau_B} \cdot \dot{\gamma} \tag{11}$$

From (4) and (11) results *the dimensionless Bingham equation*:

$$\frac{\tau}{\tau_B} = 1 + \frac{M_n}{M_n^*} \tag{12}$$

Representing the $\frac{\tau}{\tau_B} = f\left(M_n\right)$ data for all shear rates and magnetic induction values for a MRF, the data collapses on a single curve, so *a master curve* is obtained.
Such a master curve was obtained for commercial magnetorheological fluids (MRFs) and for inverse ferrofluids (IFFs) by Sherman and collab. [37], Ruiz-López and collab. [35].

2) In the case of FF-MRFs, the flow curves are no longer linear at high shear rates. The flow curves are very well described in this case by Casson's model:

$$\sqrt{\tau} = \sqrt{\tau_C} + \sqrt{\eta_C \cdot \dot{\gamma}} \tag{13}$$

where: τ_C represents the Casson yield stress, and $\eta_C =$ Casson viscosity.

It results, by squaring:

$$\tau = \tau_C + 2 \cdot \sqrt{\tau_C \cdot \eta_\infty \cdot \dot{\gamma}} + \eta_\infty \cdot \dot{\gamma} \tag{14}$$

Physical significance of Casson viscosity:

To determine the physical significance of the Casson viscosity we divide the formula (14) by $\dot{\gamma}$ and obtain:

$$\eta = \frac{\tau_C}{\dot{\gamma}} + 2 \cdot \sqrt{\frac{\tau_C \cdot \eta_C}{\dot{\gamma}}} + \eta_C \tag{15}$$

For very high shear rates:

$$\dot{\gamma} \to \infty \;\Rightarrow\; \eta_\infty = \eta_C \tag{16}$$

So the Casson viscosity has the meaning of viscosity at infinitely high shear rates.

We divide the equation (14) by the yield stress:

$$\frac{\tau}{\tau_C} = 1 + 2 \cdot \sqrt{\frac{\eta_\infty \cdot \dot{\gamma}}{\tau_C}} + \frac{\eta_\infty \cdot \dot{\gamma}}{\tau_C} \tag{17}$$

In case of FF-MRF, the Mason number and the critical Mason number are redefined for FF-MRF as follows [32], [38]:

$$M_n = 72 \frac{\eta_{FF}}{\mu_o \, \mu_{r\,FF} \left\langle M_p \right\rangle^2} \dot{\gamma} \tag{18}$$

$$M_n^* = 72 \frac{\eta_{FF}}{\mu_o \, \mu_{r\,FF} \left\langle M_p \right\rangle^2} \cdot \frac{\tau_C}{\eta_\infty} \tag{19}$$

where: n_{FF} = viscosity of FF used as carrier liquid, μ_{rFF} = relative magnetic permeability of FF.

In eq. (18) and (19) the magnetization of a suspended spherical iron microparticle is determined using data from the magnetization curves of FF-MRF and FF, with the formula [32]:

$$\left\langle M_p \right\rangle = \frac{\left\langle M_{FF-MRF} \right\rangle - \left\langle M_{FF} \right\rangle}{\Phi_{Fe}} \tag{20}$$

From formulas (18) and (19) follows:

$$\frac{M_n}{M_n^*} = \frac{\eta_\infty}{\tau_C} \cdot \dot{\gamma} \tag{21}$$

Taking into account equation (21), formula (17) becomes, as stated in [35]:

$$\frac{\tau}{\tau_C}=1+2\cdot\sqrt{\frac{M_n}{M_n^*}}+\frac{M_n}{M_n^*} \tag{22}$$

This equation represents *the dimensionless Casson equation*.

How the Casson number is defined as the ratio of magnetic forces to the viscous ones [39], [40], it is obtained:

$$C_a=\frac{\tau_C}{\eta_C\dot{\gamma}}=\frac{\tau_C}{\eta_\infty\dot{\gamma}} \tag{23}$$

and considering the relationship (21), it results:

$$\frac{M_n}{M_n^*}=\frac{1}{C_a} \tag{24}$$

The relation (22) becomes:

$$\frac{\tau}{\tau_C}=1+\frac{1}{C_a}+2\sqrt{\frac{1}{C_a}} \tag{25}$$

If the $\frac{\tau}{\tau_C}=f\left(M_n\right)$ data for all shear rates and magnetic induction values will be represented, *a master curve* will be generated for each sample of FF-MRF. If the $\frac{\tau}{\tau_C}=f\left(\frac{M_n}{M_n^*}\right)=f\left(\frac{1}{C_a}\right)$ data for samples with different volume fractions of Fe particles, at all shear rates and magnetic induction values will be represented, *the data will overlap on a single curve*, as we will show below.

3. Experimental

3.1. Samples

The samples investigated in this paper are part of one of the sets of FF-MRF analyzed in papers [32], [33]. They were prepared in the Laboratory of Magnetic Fluids of the Romanian Academy - Timisoara Branch. It started from ferrofluid F 500, which was prepared by the method of chemical coprecipitation and steric stabilization [41] and which has a very good colloidal stability. The carrier liquid is transformer oil, and the spherical magnetite particles have an average size of 6.9 nm without a chemisorbed monolayer of oleic acid, and 7.66 nm mean physical diameter, and volume fraction is 11.67%.

The 4 samples of FF-MRF (F 500-10%, F 500-20%, F 500-30%, F 500-40%) were obtained by dispersion in F500 of spherical particles of iron carbonyl with a diameter of 10 microns and density of 7.87 g/cm^3 (purchased from Merck KGaA, Darmstadt, Germany). The volume fractions and saturation magnetizations of these composite samples are specified in Table 1.

Table 1. Presentation of investigated FF-MRF samples.

Sample code	Magnetite nanoparticles volume fraction φ (%)	Iron microparticles volume fraction Φ_{Fe} (%)	Saturation magnetization *Ms* [G]
F 500-10%	11.67	10	992
F 500-20%		20	4608
F 500-30%		30	7332
F 500-40%		40	9466

3.2. Experimental setup

Rheological measurements were performed using a Physica MCR 300 rheometer (Anton Paar, Germany), with the MRD 170/1 T-SN80730989 magnetorheological cell. The gap between the parallel plates (with a 20 mm diameter) of the MR cell was fixed at 0.2 mm, and the preset temperature was 20^{o}C. In case of this cell, the magnetic field is applied perpendicular to the sample layer using a coil placed under the bottom plate of the MR cell, and the magnetic flux density in the sample was determined using a Hall probe, as described in [42].

4. Results and discussion

The magnetization curves shown in fig. 1 were measured at room temperature by Dr. Oana Balau, using a vibrating sample magnetometer – VSM 880-ADE Technologies, USA, in the field range 0 - 950 kA/m. They were used to determine the values of the magnetization at each value of the magnetic field induction for both the ferrofluid used as the carrier liquid and for each sample. With these values we calculated the average magnetization of a Fe particle at each value of the magnetic field with formula (20), and further we determined the values of Mn with formula (18).

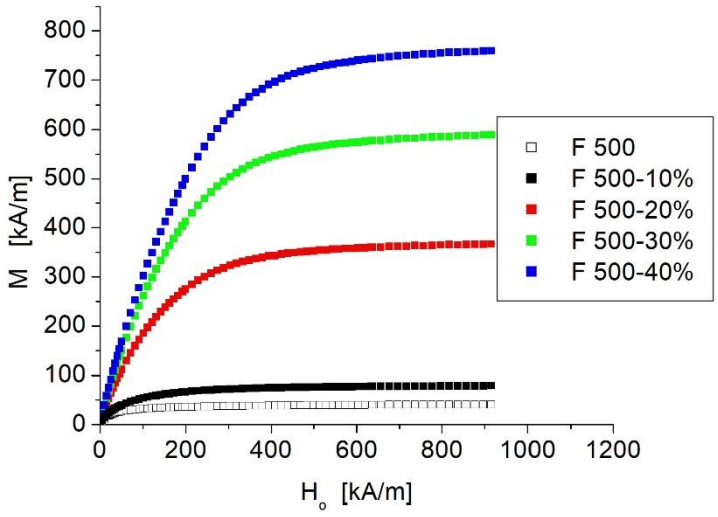

Figure 1. Magnetization curves of the ferrofluid used as the carrier liquid and of the of FF-MRF samples.

Using a Physica MCR 300, the flow curves at room temperature (t = 20°C) for eight values of magnetic field (B = 0, 25, 58, 103, 148, 220, 323, 418 mT) were measured. They were fitted with the Casson model – formula (14). E.g., fig. 2 illustrates these fits for one of the investigated samples, F500-40%. The fit parameters values τ_C and η_∞ are listed in the legend of figure 2, and they are generally increasing with the induction of the applied magnetic field, because the sample stiffens as the field intensifies.

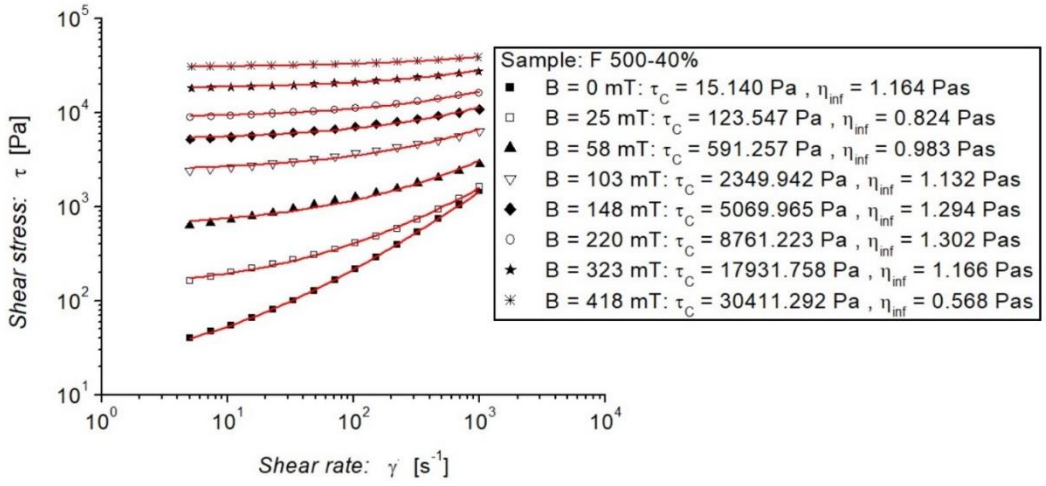

Figure 2. Flow curves at different values of magnetic field for FF 500-40% sample.
The solid lines represent the fits with Casson model.

The dependence $\frac{\tau}{\tau_C} = f\left(M_n\right)$ has been determined and it was observed that the data for each samples at all magnetic field values overlap on a single curve. This result is exemplified in fig. 3 for F 500-10% sample. The combined data sets were fitted with the dimensionless Casson equation (22). The fit value of parameter M_n^* for this sample is given in the legend of the figure.

The master curves obtained for the four samples are distinct curves, as shown in Figure 4. In this figure, the data sets measured at different values of the magnetic field were grouped and represented with a single color for each sample. The values obtained for the parameter Mn * in the case of each sample are those from the legend of the figure. As it can be observed, the parameter M_n^* decreases for increasing Fe volume fraction Φ_{Fe} (except F 500-40%), which is an explainable tendency taking into account the increase in the magnetic forces over the viscous ones due to the increase of volume fraction o Fe microparticles.

In the case of sample F 500-40% the behavior is different because the volume fraction of Fe exceeds the critical iron volume fraction (30%, as shown in [33]). The agglomerations of iron microparticles in this sample are probably more complex than those of the linear chain type, as it was also mentioned in [31], [32], [43], [44], [45].

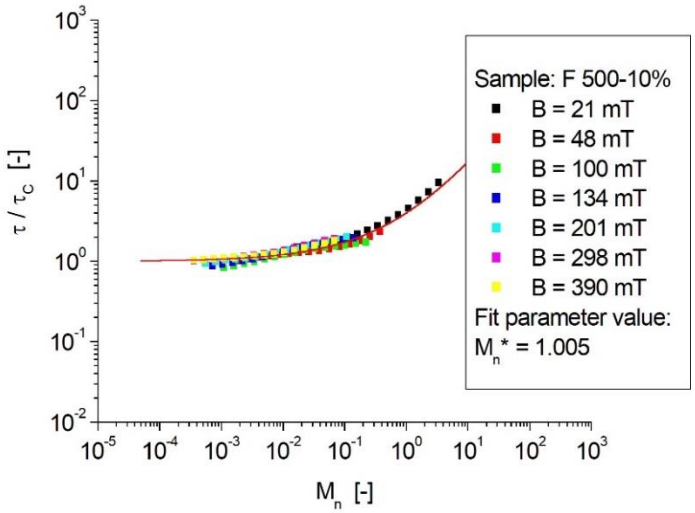

Figure 3. Non-dimensional shear stress vs. Mason number for F 500-10% sample at all the magnetic induction values. Fit line: $\frac{\tau}{\tau_C} = 1 + 2 \cdot \sqrt{\frac{M_n}{M_n^*}} + \frac{M_n}{M_n^*}$.

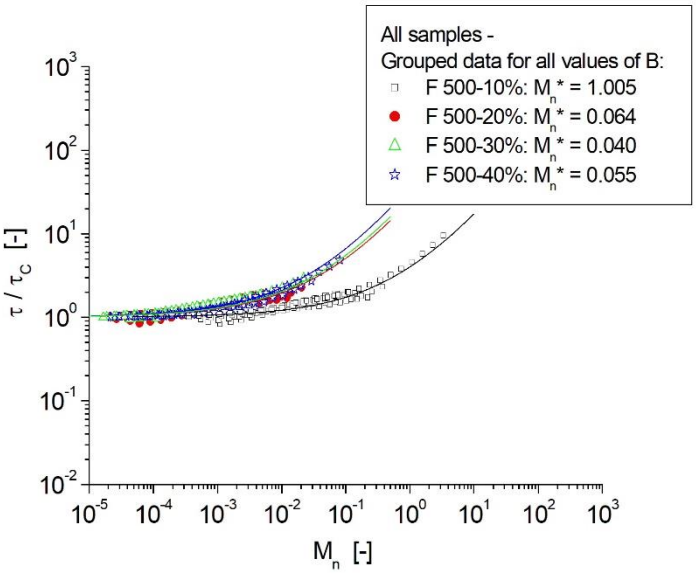

Figure 4. The master curves $\frac{\tau}{\tau_C} = f\left(M_n\right)$ for all samples.

But, representing the dependence $\frac{\tau}{\tau_C} = f\left(\frac{M_n}{M_n^*}\right) = f\left(\frac{1}{C_a}\right)$, we observe that the measured data for all samples (with different volumetric fractions of Fe microparticles), at different values of the induction of the magnetic field, a single master curve is generated - figure 5. Also, the corresponding fit lines they overlap perfectly.

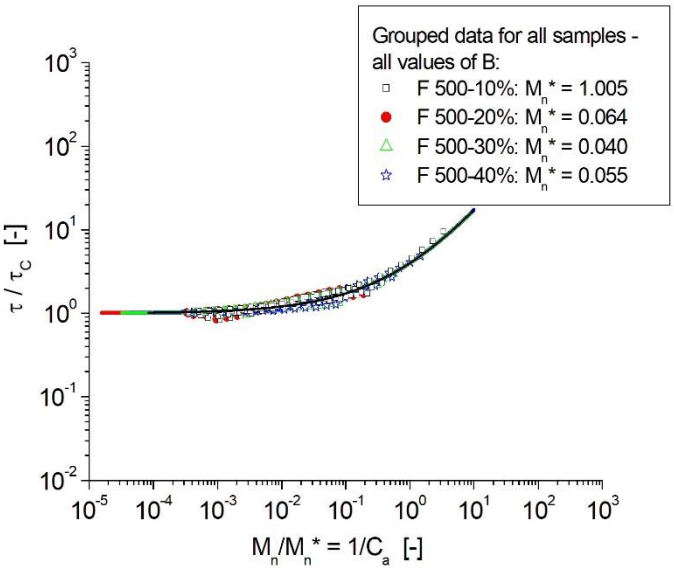

Figure 5. The dependence $\frac{\tau}{\tau_C} = f\left(\frac{M_n}{M_n^*}\right) = f\left(\frac{1}{C_a}\right)$ for all samples (al volume fraction of Fe microparticles), at all shear rates and magnetic induction values.

5. Conclusions

The magnetoreological behavior off ferrofluid-based magnetorheological fluids (FF-MRFs), especially the yield stress in the applied magnetic field is essential for the design and optimal operation of all technical (a high performance lubricant for semiactive dampers and brakes, as well as for rotating seals) or biomedical (smart prostheses for joints) applications.

In this paper it was shown that for FF-MRFs the dependence of the normalized shear stress with the Casson yield stress, simultaneously on the applied magnetic field and the shear rate, can be characterized using a single variable – either the Mason number (M_n) or the Casson number (C_a).

We investigated four samples of FF-MRF obtained by dispersing micrometric particles of Fe in different volume fractions (10, 20, 30, 40%) in a high colloidal stability ferrofluid, based on transformer oil, with magnetite nanoparticles and saturation magnetization *Ms* = 500 G. Using an MCR 300 rheometer, the flow curves in the absence and presence of a magnetic field with different values of magnetic induction were measured.

We have shown that, for a FF-MRF, if the $\frac{\tau}{\tau_C} = f\left(M_n\right)$ data for all shear rates and magnetic induction values for a FF-MRF are represented, *a master curve* is generated. More, by drawing the curves $\frac{\tau}{\tau_C} = f\left(\frac{M_n}{M_n^*}\right) = f\left(\frac{1}{C_a}\right)$ for all samples (with different volume fractions of Fe microparticles), at all shear rates and magnetic induction values, *the data* collapse on a master curve.

The utility of these master curves: Using of such master curve, the optimal concentrations of microparticles of the bidispersed composites can be determined for the control of their magnetoreological behavior, so that in specific operating conditions to obtain high-performance practical applications.

Acknowledgements

The authors are grateful to Florica Balanean, Research Assistant (Laboratory of Magnetic Fluids-Center for Fundamental and Advanced Technical Research, Romanian Academy-Timisoara Branch) for preparing the ferrofluid carriers and the nanomicro composite MR fluid samples , and to Dr. Oana Marinica (RCHCF-University Politehnica Timisoara) for magnetization measurements.

References

[1] Klingenberg D.J., *Magnetorheology: applications and challenges*, AIChE J **47**(2):246–249 (2001), Doi: 10.1002/aic.690470202.

[2] Carlson J.D. and Jolly M.R., *MR Fluid, foam and elastomer devices*, Mechatronics **10**:555–569 (2000), Doi: 0.1016/S0957-4158(99)00064-1.

[3] de Vicente J., Klingenberg D.J., Hidalgo-Álvarez R., *Magnetorheological fluids: a review,* Soft Matter **7**:3701–3710 (2011), doi:10.1039/c0sm01221a.

[4] Portillo M.A., Lozada P.S.A., Figueroa I.A., Suarez M.A., Delgado A.V.C. and Iglesias G.R., *Synergy between magnetorheological fluids and aluminum foams: Prospective alternative for seismic damping*, Journal of Intelligent Material Systems and Structures, **27**:872–879 (2016), Doi: 10.1177/1045389X15596624.

[5] Szakal R., Susan-Resiga D., Muntean S., Vékás L., *Magnetorheological Fluids Flow Modelling Used in a Magnetorheological Brake Configuration*, Proc. of 2019 International Conference on ENERGY and ENVIRONMENT (CIEM), Timișoara, Romania, Article No. 19228489, pg. 403-407 (2019 a), Doi: 10.1109/CIEM46456.2019.8937624.

[6] Szakal R.-A., Bosioc A.I., Muntean S., Susan-Resiga D., Vékás L, *Experimental Investigations of a Magneto-Rheological Brake Embedded in a Swirl Generator Apparatus,* capitol in Silva L. (eds) Materials Design and Applications II. Advanced Structured Materials, Springer, **98**:265-279 (2019 b), Doi:10.1007/978-3-030-02257-0_20.

[7] Carlson J.D. and Sproston J.L., *Controllable Fluids in 2000 - Status of ER and MR Fluid Technology*, Proceedings of Actuator 2000-8th Int. Conf on New Actuators, Bremen, Germany, 126-130 (2000).

[8] Liu J., Flores G.A. and Sheng R., *In-vitro investigation of blood embolization in cancer treatment using magnetorheological fluids*, Journal of Magnetism and Magnetic Materials, **225**(1-2):209-217 (2001), Doi: 10.1016/S0304-8853(00)01260-9.

[9] Susan-Resiga D. and Barvinschi P., *Nano-microstructured magnetorheological fluids and engineering applications,* Romanian Journal of Technical Sciences – Applied Mechanics, 65(2): 87-121 (2020).

[10] Susan-Resiga, *Aspecte ale comportării reologice a fluidelor magnetizabile*, Teză de abilitare, Universitatea de Vest din Timişoara (2020).

[11] Skjeltorp A.T., *One- and Two-Dimensional Crystallization of Magnetic Holes*, Physical Review Letters 51:2306–2309 (1983), Doi: 10.1103/PhysRevLett.51.2306.

[12] Popplewell J., Rosensweig R.E., *Magnetorheological fluid composites*, J. Phys. D. Appl.Phys., **29**(9):2297-2303 (1996), Doi: 10.1088/0022-3727/29/9/011.

[13] de Gans B.J., Duin N.J., van den Ende D., and Mellema J., *The influence of particle size on the magnetorheological properties of an inverse ferrofluid*, Journal of Chemical Physics **113**(5):2032-2042 (2000), Doi: 10.1063/1.482011.

[14] van Ewijk G., *Phase behavior of mixtures of magnetic colloids and non-adsorbing polymer*, PhD thesis, University of Utrecht (2001).

[15] de Vicente J., López-López M.T., González-Caballero F., Durán J.D.G., *Rheological study of the stabilization of magnetizable colloidal suspensions by addition of silica nanoparticles*, Journal of Rheology **47**:1093 (2003), Doi: 0.1122/1.1595094.

[16] López-López M.T., Zugaldía A., González-Caballero F. and Durán J.D.G., *Sedimentation and redispersion phenomena in iron-based magnetorheological fluids*, Journal of Rheology **50**(4):543-560 (2006 a), Doi: 10.1122/1.2206716.

[17] Choi C.-I., Xie L., Wereley N.M., *Testing and analysis of magnetorheological fluid sedimentation in a column using a vertical axis inductance monitoring system*, Smart Matererials and Structures **25**(4):04LT01 (2016), Doi: 0.1088/0964-1726/25/4/04LT01.

[18] Socoliuc V., Vékás L. and Turcu R., *Magnetically induced phase condensation in an aqueous dispersion of magnetic nanogels*, Soft Matter **9**:3098–3105 (2013), Doi: 10.1039/C2SM27262H.

[19] Rosenfeld N.C., Wereley N.M., Radhakrishnan R. and Sudarshan T., *Behavior of Magnetorheological Fluids Utilizing Nanopowder Iron*, International Journal of Modern Physics B **16**(17–18):2392–2398 (2002), Doi: 10.1142/S0217979202012414.

[20] Wereley N.M., Chaudhuri A., Yoo J.-H., John S., Kotha S., Suggs A., Radhakrishnan R., Love B.J., Sudarshan T.S., *Bidisperse magnetorheological fluids using Fe particles at nanometer and micron scale*, Journal of Intelligent Material Systems and Structures **17**(5):393–401 (2006), Doi:10.1177/1045389X06056953.

[21] Morillas J.R., Bombard J.F. and de Vicente J., *Enhancing magnetorheological effect using bimodal suspensions in the single-multidomain limit*, Smart Materials and Structures **27**(7):07LT01 (2018), Doi: 10.1088/1361-665X/aac8ae.

[22] Lim S.T., Cho M.S., Jang I.B., Choi H.J., Jhon M.S., *Magnetorheology of Carbonyl-Iron Suspensions With Submicron-Sized Filler*, IEEE Transactions on Magnetics **40**(4):3033 – 3035 (2004), Doi: 10.1109/TMAG.2004.830400.

[23] de Vicente J., Segovia-Gutiérrez J.P., Andablo-Reyes E., Vereda F., *Dynamic rheology of sphere- and rod-based magnetorheological fluids*, The Journal of Chemical Physics **131**(19):194902 (2009), Doi: 10.1063/1.3259358.

[24] Vereda F., de Vicente J., Segovia-Gutiérrez J.P., Hidalgo-Alvarez R., *Average particle magnetization as an experimental scaling parameter for the yield stress of dilute magnetorheological fluids*, Journal of Physics D: Applied Physics **44**(42):425002 (2011), Doi:10.1088/0022-3727/44/42/425002.

[25] Shah K., Phu D.X., Seong M.-S., Upadhyay R.V. and Choi S.-B., *A low sedimentation magnetorheological fluid based on platelike iron particles, and verification using a damper test*, Smart Materials and Structures **23**(2):027001 (2014), Doi: 10.1088/0964-1726/23/2/027001.

[26] Susan-Resiga D. and Vékás L., *From high magnetization ferrofluids to nano-micro composite magnetorheological fluids: properties and applications*, Romanian Reports in Physics **70**:501 (2018).

[27] López-López M.T., de Vicente J., Bossis G., González-Caballero F., and Durán J.D.G., *Preparation of stable magnetorheological fluids based on extremely bimodal iron–magnetite suspensions*, Journal of Materials Research **20** (4), 874–881 (2005), Doi: 10.1557/JMR.2005.0108.

[28] López-López M.T., Kuzhir P., Lacis S., Bossis G., González-Caballero F., and Durán J.D.G., *Magnetorheology for suspensions of solid particles dispersed in ferrofluids*, Journal of Physics: Condensed Matter **18**(38):S2803–S2813 (2006 b), Doi: 0.1088/0953-8984/18/38/S18.

[29] Yang Y., Li L. and Chen G., *Static yield stress of ferrofluid-based magnetorheological fluids*, Rheol. Acta **48**(4):457–466 (2009), Doi: 0.1007/s00397-009-0346-z.

[30] Marinică O., Susan-Resiga D., Bălănean F., Vizman D., Socoliuc V., Vékás L., *Nano-microcomposite magnetic fluids: Magnetic and magnetorheologica levaluation for rotating seal and vibration damper applications*, Journal of Magnetism and Magnetic Materials 406:134–143 (2016), Doi: 10.1016/j.jmmm.2015.12.095.

[31] Susan-Resiga D. and Vékás L., *Ferrofluid-based magnetorheological fluids: Tuning the properties by varying the composition at two hierarchical levels*, Rheologica Acta **55**(7), 581–595 (2016), Doi: 10.1007/s00397-016-0931-x.

[32] Susan-Resiga D. and Vékás L., *Ferrofluid based composite fluids: Magnetorheological properties correlated by Mason and Casson numbers*, Journal of Rheology **61**(3), 401 - 408 (2017), Doi: 10.1122/1.4977713.

[33] Susan-Resiga D. and Barvinschi P., *Correlation of rheological properties of ferrofluid-based magnetorheological fluids using the concentration-magnetization superposition*, Journal of Rheology **62**(3), 739 - 752 (2018), Doi: 10.1122/1.5017674.

[34] Bingham E. C. and Green H., *Plastic Material and not a Viscous Liquid; The Measurement of its Mobility and yield value*. Proc. Amer. Soc. Test Mater (1919).

[35] Ruiz-López J. A., Fernández-Toledano J. C., Hidalgo-Alvarez R., J. de Vicente, *Testing the mean magnetization approximation, dimensionless and scaling numbers in magnetorheology*, Soft Matter, **12**, 1468 - 1476 (2016).

[36] Klingenberg D. J., Ulicny J. C., Golden M. A., *Mason numbers for magnetorheology*, Journal of Rheology, **51**(5), 883 - 893 (2007).

[37] Sherman S.G., Becnel A.C., Wereley N.M., *Relating Mason number to Bingham number in magnetorheological fluids*, Journal of Magnetism and Magnetic Materials, **380**, 98-104 (2015).

[38] Vălu Gh. O., *Aspecte ale magnetoreologiei fluidelor magnetizabile*, Lucrare de licență, Universitatea de Vest, 2020.

[39] Pham V. and Mitsoulis E., *Entry and Exit Flows of Casson Fluids*, The Canadian Journal of Chemical Engineering **72**(6):1080 – 1084 (1994), Doi: 10.1002/cjce.5450720619.

[40] Casson N., *A Flow Equation for Pigment-Oil Suspensions of the Printing Ink Type*, In: Mill C.C., Ed., Rheology of Disperse Systems, Pergamon Press, Oxford, 84-104 (1959).

[41] Bica D., Potencz I., Vékás L. , Giula G., and Potra (Balanean) F., *Procedure to obtain magnetic fluids for seals*, Romanian Patent No. RO 115533:B1 (2000).

[42] Laun H. M., Schmidt G., Gabriel C., and Kieburg C., *Reliable plate–plate MRF magnetorheometry based on validated radial magnetic flux density profile simulations*, Rheologica Acta 47(9), 1049–1059 (2008).

[43] Shulman Z.P., Kordonskii V.I., Zaltsgendler E.A., Prokhorov I.V., Khusid B.M., and Demchuk S.A., *Dynamic and physical properties of ferrosuspensions with a structure rearranged by an external magnetic field*, Magnetohydrodynamics **20**, 354–361 (1984).

[44] Bossis G., Lemaire E., Volkova O., and Clercx H., *Yield stress in magnetorheological and electrorheological fluids: A comparison between microscopic and macroscopic structural models*, Journal of Rheology 4**1**, 687–704 (1997), Doi: 10.1122/1.550838.

[45] Gómez-Ramírez A., Kuzhir P., Lopez-Lopez M.T., Bossis G., Meunier A., and Duran J.D.G., *Steady shear flow of magnetic fiber suspensions: Theory and comparison with experiments*, Journal of Rheology **55**, 43–67 (2011), Doi: 10.1122/1.3523477.